THE JOURNAL OF BIOLOGICAL CHEMISTRY
Vol. 276, No. 47, Issue of November 23, pp. 44247–44257, 2001
Printed in U.S.A.

AKAP-Lbc Anchors Protein Kinase A and Nucleates $G\alpha_{12}$-selective Rho-mediated Stress Fiber Formation*

Received for publication, July 16, 2001, and in revised form, September 5, 2001
Published, JBC Papers in Press, September 6, 2001, DOI 10.1074/jbc.M106629200

Dario Diviani, Jacquelyn Soderling, and John D. Scott‡

From the Howard Hughes Medical Institute, Vollum Institute, Oregon Health Sciences University, Portland, Oregon 97201

Guanine nucleotide exchange factors of the Dbl family relay signals from membrane receptors to Rho family GTPases. We now demonstrate that a longer transcript of the Lbc gene encodes a chimeric molecule, which we have called AKAP-Lbc, that functions as an A-kinase-anchoring protein (AKAP) and a Rho-selective guanine nucleotide exchange factor. Expression of AKAP-Lbc in fibroblasts favors the formation of stress fibers in a Rho-dependent manner. Application of lysophosphatidic acid or selective expression of $G\alpha_{12}$ enhances cellular AKAP-Lbc activation. Furthermore, biochemical studies indicate that AKAP-Lbc functions as an adaptor protein to selectively couple $G\alpha_{12}$ to Rho. Thus, AKAP-Lbc anchors PKA and nucleates the assembly of a Rho-mediated signaling pathway.

The transmission of information from the plasma membrane to the actin cytoskeleton is essential to control a variety of dynamic cellular processes including cell shape, motility, and adherence (1). Critical mediators of these events are the Rho family small molecular weight GTPases, Rho, Rac, and Cdc42, which regulate distinct actin remodeling events. Rho is primarily responsible for the assembly of actin stress fibers and focal adhesions, and Rac controls the formation of lamellipodia, while Cdc42 induces filopodial formation (1, 2). In addition to these effects, Rho has also been implicated in a variety of other critical cellular functions including gene transcription (3, 4) and progression through the cell cycle (5).

Lysophosphatidic acid (LPA) and thrombin are the extracellular ligands that induce Rho signaling events (2). Binding of either ligand to distinct classes of cell surface receptors triggers a series of events that mobilize the pertussis toxin-insensitive heterotrimeric G protein subunits $G\alpha_{12}$ and $G\alpha_{13}$ (6, 7). The intracellular targets for either $G\alpha$ subunit are a growing family of guanine nucleotide exchange factors (GEFs) (8). These exchange factors dock with activated $G\alpha_{12}$ and $G\alpha_{13}$ and facilitate GTP loading of Rho. Individual cells express several Rho-GEFs, which activate distinct Rho signaling pathways (9). For example, p115 Rho-GEF interacts with $G\alpha_{13}$ through a regulator of G protein signaling (RGS) domain located in the amino-terminal region of the exchange factor (10, 11). Likewise, a related module, the Lsc homology domain, governs docking of $G\alpha_{13}$ to exchange factors such as PDZ Rho-GEF, KIAA0380, or GTRAP48 (12–14).

A universal hallmark of exchange factors that activate GTPases of the Rho family is a conserved region of ~250 residues that contains a Dbl homology (DH) domain followed by a pleckstrin homology domain (9). The DH domain contains the nucleotide exchange activity, whereas the pleckstrin homology domain is thought to be involved in the subcellular localization of GEFs (2). GTPase selectivity is governed by determinants located within the DH domain that discriminate Rho-specific from Rac or Cdc42-specific exchange factors. Several families of Rho-specific exchange factors have been recognized. Members of the Lbc family were originally identified in a screen for transforming genes from human myeloid leukemias (15). Onco-Lbc is a 424-residue oncogenic protein with unregulated exchange factor activity that transforms NIH-3T3 cells in a Rho-dependent manner (16). Subsequently, a proto-oncogenic form has been isolated with a COOH-terminal region that attenuates its transforming potential (17). More recently, a splice variant called Brx has been identified that is specifically expressed in testis and estrogen-sensitive tissues (18). Interestingly, Lbc does not possess RGS-like domains, suggesting that different mechanisms might be involved in its activation in response to extracellular signals.

In this study, we demonstrate that a novel Lbc splice variant, AKAP-Lbc, is also an A-kinase-anchoring protein (AKAP). AKAPs are a group of functionally related proteins that coordinate cAMP-responsive events at defined subcellular compartments by directing PKA toward preferred substrates (19–21). Many AKAPs contain distinct binding sites for PKA and other signaling enzymes such as phosphatases (19), phosphodiesterases (22), and other protein kinases (23–26). Through modular interactions, multienzyme complexes are assembled at specific sites in the cell to process and integrate various signals. For a decade, a PKA binding fragment called Ht31 has served as the prototype for a structural elucidation of how the PKA holoenzyme interacts with AKAPs (27, 28). We now show that the original Ht31 fragment is part of a larger molecule with Rho-specific guanine nucleotide exchange activity. Cell-based experiments demonstrate that AKAP-Lbc nucleates a $G\alpha_{12}$-mediated Rho activation pathway that responds to LPA.

EXPERIMENTAL PROCEDURES

Cloning of AKAP-Lbc—A 3045-base pair cDNA clone encoding for an RII-binding protein fragment designated as Ht31 was originally isolated from a human thyroid expression library (29). The sequence upstream of the Ht31 clone was isolated by rapid amplification of cDNA ends using human heart marathon-adapted cDNA (CLONTECH). To isolate a full-length AKAP-Lbc cDNA, human heart poly(A)$^+$ mRNA was reverse-transcribed using a reverse primer corresponding to nucleotides 4302–4330 of the proto-Lbc cDNA. The resulting cDNA was PCR-amplified using specific primers and subcloned into pCDNA3 or pEGFP. Three independent PCR products encompassing the entire AKAP-Lbc cDNA were sequenced in both directions.

Northern Blots—DNA probes were radiolabeled with [α-^{32}P]dCTP to

* This work was supported by National Institutes of Health Grant DK44239 (to J. D. S.). The costs of publication of this article were defrayed in part by the payment of page charges. This article must therefore be hereby marked "*advertisement*" in accordance with 18 U.S.C. Section 1734 solely to indicate this fact.

The nucleotide sequence(s) reported in this paper has been submitted to the GenBank™/EBI Data Bank with accession number(s) AF406992.

‡ To whom correspondence should be addressed: Howard Hughes Medical Institute, Vollum Institute, Oregon Health Sciences University, 3181 S.W. Sam Jackson Park Rd., Portland, OR 97201. Tel.: 503-494-4656; Fax: 503-494-0519; E-mail: scott@ohsu.edu.

a specific activity of 10^9 cpm/μg of DNA. Multiple Tissue Northern blots (CLONTECH) were hybridized using a probe corresponding to nucleotides 1–500 of the AKAP-Lbc cDNA according to the manufacturer's protocol.

Expression Constructs—The A1251P/I1260P and Y2153F mutants of AKAP-Lbc were generated using the QuikChange mutagenesis method (Stratagene). The RhoA, Rac1, and Cdc42 expression constructs were provided by Andrew Thorburn. The G14V and T19N mutations in the NH_2 terminus of RhoA were made using the QuikChange mutagenesis method (Stratagene). The FLAG-tagged RhoA, RhoB, and RhoC constructs were generously provided by Melvin Simon. For the construction of the GST fusion protein of the Rho-binding domain (RBD) of rhotekin, the RBD was PCR-amplified from mouse brain cDNA (CLONTECH) and subcloned into pGEX-4T. The expression constructs for the constitutively active mutants of $G\alpha_{12}$, $G\alpha_{13}$, $G\alpha_q$, $G\alpha_{11}$, $G\alpha_{i2}$, and $G\alpha_s$ were obtained form the Guthrie cDNA Resource Center. The dominant negative mutants of $G\alpha_{12}$ and $G\alpha_{13}$ were generated using the QuikChange mutagenesis method (Stratagene).

Antibodies—Antibodies to AKAP-Lbc were generated in rabbits using a recombinant His_6-tagged AKAP-Lbc protein fragment (residues 789–1186) as the immunogen. Affinity purification of this antiserum was accomplished using the immunogen immobilized on Affi-Gel 15 resin (Bio-Rad) and following the manufacturer's instructions.

AKAP-Lbc serum was used at a 1:200 dilution for immunoprecipitations and at a 1:5000 dilution for immunoblots, whereas affinity-purified AKAP-Lbc antibodies were used at a concentration of 10 μg/ml for immunoprecipitations and 1 μg/ml for immunoblots.

The following affinity-purified primary antibodies were used for immunoblotting: rabbit polyclonal antibody to RhoA (200 μg/ml, 1:250 dilution; Santa Cruz Biotechnology, Inc., Santa Cruz, CA); mouse monoclonal antibodies to RhoA, Rac1, or Cdc42 (200 μg/ml, 1:250 dilution; Santa Cruz Biotechnology); mouse monoclonal antibody to PKA catalytic subunit (clone 5B, 1:1000 dilution; Transduction Laboratories); mouse monoclonal to PKA type II regulatory subunit (1:250 dilution; Transduction Laboratories); mouse monoclonal antibody to the GST tag (1:500 dilution; Santa Cruz Biotechnology); mouse monoclonal antibody to the FLAG tag (1:2000 dilution; Sigma); rabbit polyclonal antibody to the GFP tag (1:100 dilution; Invitrogen); rabbit polyclonal antibody to $G\alpha_{12}$ (1:500 dilution; Santa Cruz Biotechnology); rabbit polyclonal antibody to $G\alpha_{13}$ (1:250 dilution; Santa Cruz Biotechnology); rabbit polyclonal antibody to $G\alpha_q$ (1:500 dilution; Santa Cruz Biotechnology); rabbit polyclonal antibody to $G\alpha_{11}$ (1:500 dilution; Santa Cruz Biotechnology); rabbit polyclonal antibody to $G\alpha_{i2}$ (1:500 dilution; Santa Cruz Biotechnology); and rabbit polyclonal antibody to $G\alpha_s$ (1:500 dilution; Santa Cruz Biotechnology).

Purification of Recombinant Proteins—RhoA, Rac1, and Cdc42 and the Rho-binding domain of rhotekin were expressed as NH_2-terminal GST fusion proteins in bacteria (BL21DE3) (30). Recombinant proteins expressed in bacteria were purified using glutathione-Sepharose (Amersham Pharmacia Biotech). Bacterial extracts containing GST fusion proteins were prepared by centrifugation of bacterial cultures; lysis of pelleted bacteria in 20 mM Tris, 50 mM NaCl, 5 mM $MgCl_2$, 0.5% (w/v) Triton X-100, 1 mM benzamidine, 2 μg/ml leupeptin, 2 μg/ml pepstatin; sonication; and centrifugation at 38,000 $\times$ *g* for 30 min at 4 °C. The supernatant was incubated with glutathione-Sepharose beads (Amersham Pharmacia Biotech) overnight. The resin was washed with 10 bed volumes of lysis buffer and stored at 4 °C. GST fusion proteins were eluted from the resin with 5 mM reduced glutathione for 15 min at room temperature and dialyzed.

Cell Culture and Transfection—HEK293 cells were transfected at 50–80% confluence using the LipofectAMINE Plus Reagent kit (Life Technologies, Inc.) with 0.1–6 μg of the various cDNA expression vectors. Cells were incubated with the DNA for 5 h in serum-free Dulbecco's modified Eagle's medium at 37 °C under 5% CO_2 and further incubated for 24–72 h in normal growth medium (Dulbecco's modified Eagle's medium, 10% fetal bovine serum, 1% penicillin, 1% streptomycin) before harvesting.

Extract Preparations and Immunoprecipitations—For immunoprecipitation of AKAP-Lbc complexes from heterologous expression systems, cells grown in 100-mm dishes were transfected at 70–80% confluence using 6 μg of AKAP-Lbc cDNA. Cells were harvested and lysed 24 h after transfection in 500 μl of IP buffer (10 mM phosphate, 150 mM NaCl, 5 mM EDTA, 5 mM EGTA, 1 mM benzamidine, 10 μg/ml pepstatin, 10 μg/ml leupeptin, and 1 mM 4-(2-aminoethyl)-benzenesulfonyl fluoride) containing 1% Triton X-100 and 0.2% sodium deoxycholate and then incubated for 4 h at 4 °C. Lysates were spun at 100,000 $\times$ *g* for 30 min and dialyzed twice against lysis buffer without deoxycholate. Supernatants were incubated with 5 μg of antibody or control nonimmune IgG and 40 μl of protein A- or G-agarose beads. Following overnight incubation at 4 °C, the immunocomplexes were pelleted by centrifugation (3000 $\times$ *g*, 1 min); washed four times with lysis buffer plus 650 mM NaCl, twice with lysis buffer, and twice with PBS; and eluted with 2$\times$ SDS-PAGE sample buffer. Bound proteins were analyzed by immunoblotting. For immunoprecipitation of AKAP-Lbc from human tissues or HeLa cells, extracts were processed as described above.

To detect PKA catalytic activity in AKAP-Lbc immunoprecipitates, immunocomplexes were incubated with 1 mM cAMP for 10 min. PKA catalytic activity in eluates was assayed using Leu-Arg-Arg-Ala-Ser-Leu-Gly (Kemptide) as substrate as described (31). PKA activity was defined as the activity inhibited by the PKI-(5–24) inhibitor peptide.

Immunoblots and Solid Phase [^{32}P]RII Overlays—For immunoblots, the nitrocellulose filters were blocked overnight with Blotto plus 0.1% bovine serum albumin in TBS (100 mM Tris, pH 7.4, 140 mM NaCl, and 5% nonfat dry milk) at room temperature, washed three times with TTBS (0.05% Tween 20 in TBS), and then incubated with the specific primary antibody diluted in TTBS for 2 h at room temperature. After three washes with TTBS, filters were probed with horseradish peroxidase-conjugated secondary antibody (Amersham Pharmacia Biotech) in TTBS for 1 h, washed with TBS, and developed using the enhanced chemiluminescence method according to the manufacturer's protocol (Amersham Pharmacia Biotech). For [^{32}P]RII overlays, the filters were blocked 1 h with Blotto plus 1% bovine serum albumin in TBS at room temperature and then incubated 4–16 h with 100,000 cpm/ml PKA-phosphorylated [^{32}P]RII in Blotto plus 0.1% bovine serum albumin. After extensive washes in TTBS, the blots were visualized by autoradiography.

AKAP-Lbc Pull-down Assays—HEK293 cells grown in 100-mm dishes were transfected with 6 μg of the AKAP-Lbc/pEGFP or AKAP-Lbc Y2153F/pEGFP constructs. 24 h after transfection, cells were lysed in IP buffer containing 5 mM $MgCl_2$, 1% Triton X-100, and 0.2% sodium deoxycholate. Lysates were then centrifuged at 100,000 $\times$ g for 30 min at 4 °C and incubated overnight with a polyclonal anti-AKAP-Lbc antibody and Protein A-Sepharose at 4 °C. Beads were then washed four times in IP buffer with 650 mM NaCl and twice in IP buffer. Beads were subsequently incubated with 0.5 μg of GST-RhoA, GST-Rac1, or GST-Cdc42 previously loaded with GDP or GTPγS or nucleotide-depleted for 4 h at 4 °C. After five washes in IP buffer with 1% (w/v) Triton X-100, proteins were eluted with Laemmli buffer and separated by SDS-PAGE.

GDP/GTP Exchange Assays—The exchange assays were performed as previously described (32). For GTPγS binding, 2 μg of the recombinant GTPases were initially incubated for 5 min in 60 μl of loading buffer (20 mM Tris-HCl, pH 8.0, 100 mM NaCl, 2 mM EDTA, 0.2 mM dithiothreitol, 100 μM AMP-PNP, and 10 μM GDP) at room temperature. $MgCl_2$ was then added to a final concentration of 5 mM, and the incubation continued for an additional 15 min. Finally, aliquots (20 μl) of GDP-loaded GTPases were mixed with 100 μg of lysates from cells overexpressing either AKAP-Lbc or AKAP-Lbc Y2153F diluted in reaction buffer (20 mM Tris-HCl, pH 8.0, 100 mM NaCl, 10 mM $MgCl_2$, 100 μM AMP-PNP, 0.5 mg/ml bovine serum albumin, and 5 μM [^{35}S]GTPγS (11,000 cpm/pmol)) to initiate the exchange reaction (final volume 100 μl) at room temperature. Aliquots (15 μl) of samples were taken at various time points from the reaction mixture and added to 10 ml of ice-cold PBS. Bound and free nucleotides were separated by filtration through BA85 nitrocellulose filters. For the GDP dissociation assay, 10 μM radiolabeled [^{3}H]GDP was used in the loading buffer instead of GDP, and 1 mM GTP was used in the reaction buffer instead of [^{35}S]GTPγS.

RBD Pull-down Assays—HEK293 cells grown in 100-mm dishes were transfected with 6 μg of the AKAP-Lbc/pEGFP or AKAP-Lbc Y2153F/pEGFP constructs. 24 h after transfection, cells were lysed in RBD lysis buffer (50 mM Tris, pH 7.2, 1% (w/v) Triton X-100, 0.5% sodium deoxycholate, 0.1% (w/v) SDS, 500 mM NaCl, 10 mM $MgCl_2$, 1 mM benzamidine, 10 μg/ml leupeptin, 10 μg/ml aprotinin, 1 mM 4-(2-aminoethyl)-benzenesulfonyl fluoride). Lysates were subjected to centrifugation at 38,000 $\times$ *g* for 15 min at 4 °C and incubated with 30 μg of RDB beads for 45 min at 4 °C. Beads were then washed three times with RBD buffer without deoxycholate, resuspended in 2$\times$ Laemmli buffer, and analyzed by SDS-PAGE.

Confocal Microscopy—Cells grown on coverslips were transfected at 40% confluence using the LipofectAMINE Plus Reagent kit (Life Technologies, Inc.), washed twice with PBS, and then fixed for 10 min in PBS plus 3.7% formaldehyde and permeabilized for 5 min with 0.2% (w/v) Triton X-100 in PBS. Cells were blocked for 30 min in PBS plus 1% bovine serum albumin and then incubated for 1 h either with a 1:1000 dilution of polyclonal anti-AKAP-Lbc followed by 1 h in fluorescein

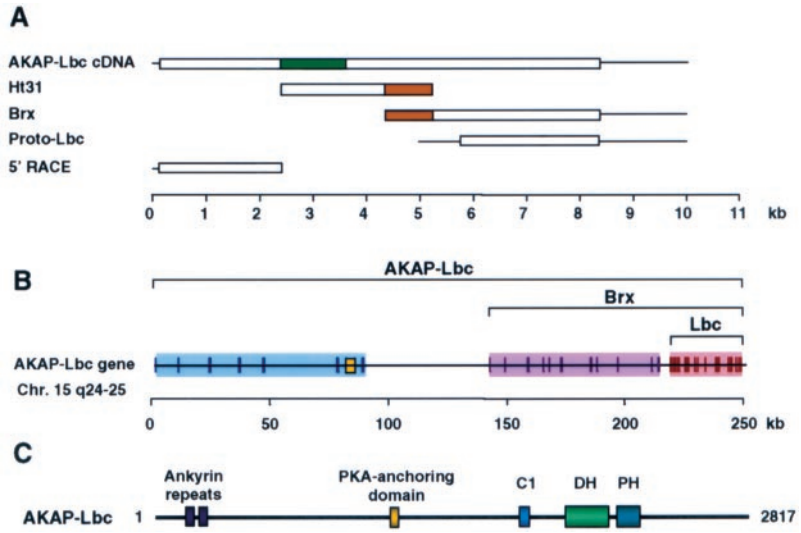

FIG. 1. **Cloning and genomic organization of AKAP-Lbc.** *A*, alignment of cDNAs corresponding to Ht31, Brx, and Proto-Lbc. 5′ rapid amplification of cDNA ends was employed to isolate cDNAs with sequence upstream of Ht31 and to identify the start of the putative human AKAP-Lbc cDNA. A full-length AKAP-Lbc cDNA of 10.1 kb with an open reading frame of 8451 was amplified from human heart poly(A)$^+$ mRNA by reverse transcriptase-PCR. Open reading frames are represented by *boxes*, and the 5′- or 3′-untranslated sequences are indicated by *lines*. The overlapping sequences of AKAP-Lbc and Brx are indicated (*red box*). The region used for the antibody production (residues 769–1168) is indicated in *green*. *B*, organization of the AKAP-Lbc gene. Exons are represented by *vertical lines* and drawn to scale. Exon 8 containing the PKA anchoring site is indicated (*yellow*). *C*, schematic representation and protein domain organization of AKAP-Lbc. The two ankyrin repeats (residues 166–224), the RII-binding domain (residues 1236–1257), the C1 homology region (residues 1792–1830), and the Dbl (*DH*) (residues 1998–2190) and pleckstrin (*PH*) (residues 2232–2335) homology domains are shown.

isothiocyanate-conjugated secondary antibody (Jackson ImmunoResearch) and Texas-red phalloidin (Molecular Probes, Inc., Eugene, OR) or Texas Red phalloidin alone. The cells were mounted using Prolong (Molecular Probes). Immunofluorescent staining or intrinsic GFP fluorescence was visualized on a laser-scanning confocal microscope (Bio-Rad).

RESULTS

Cloning of AKAP-Lbc—The Ht31 cDNA represents a partial clone encoding a 1015-amino acid PKA binding fragment that has proved to be a valuable tool for defining the molecular mechanism of PKA anchoring (29). The identity and function of the full-length anchoring protein are unknown. A data base search of GenBank™ revealed that residues 631–1015 of Ht31 were identical to the amino terminus of Brx (18), a recently identified splice variant of the guanine nucleotide exchange factor Lbc (Fig. 1*A*). Lbc variants include Brx, the oncogene, onco-Lbc, and a proto-oncogene called proto-Lbc (15, 17, 18). Our data now suggest that a fourth and larger transcript exists that includes the Ht31 sequence (Fig. 1*A*). This was confirmed by the PCR amplification of a 6693-base pair fragment encompassing the 5′ coding region of Ht31 and the 3′-untranslated sequence of proto-Lbc (Fig. 1*A*). A further 2800 base pairs of message was obtained by 5′ rapid amplification of cDNA ends, and a full-length cDNA of 10.1 kb was amplified by reverse transcriptase-PCR (Fig. 1*A*). Three independent PCR products were sequenced in both directions, revealing a coding sequence of 8451 nucleotides, encoding a protein of 2817 amino acids with a predicted molecular mass of 312 kDa (Fig. 1*C*). On the basis of the homology with Lbc, we have named this anchoring protein AKAP-Lbc. The sequence has been deposited in GenBank™ (accession number AF406992).

The AKAP-Lbc gene includes 37 exons and spans a region of 250 kb on chromosome 15 q24–25. Exons 1–9 encode unique sequences including the PKA-anchoring region, exons 10–20 encode sequences that are shared by AKAP-Lbc and Brx, and exons 21–37 encode a common region present all Lbc splice variants (Fig. 1*B*). Several protein interaction modules are present including ankyrin repeats, the RII-binding domain, and a cysteine-rich motif homologous to the C1 region of PKC (Fig. 1*C*). The carboxyl-terminal region contains a Dbl homology and a pleckstrin homology domain that are characteristic of Rho family GEFs (9) (Fig. 1*C*).

The Cellular and Subcellular Distribution of AKAP-Lbc—Earlier Northern blot analyses of Lbc mRNA tissue distribution revealed a variety of Lbc transcripts ranging from 6 to 10 kb in most human tissues (15, 17, 18). A consistent 5-kb band corresponding to Brx was specifically detected in the testis (18), whereas a single 10-kb band was detected in the heart. Here, using a probe specific to the 5′ region of the AKAP-Lbc coding sequence, a single mRNA transcript of 10 kb was predominantly detected in the heart, although lower levels of this message were evident in the lung, placenta, kidney, pancreas, skeletal muscle, and liver (Fig. 2*A*, *left panel*). AKAP-Lbc message was also detected in HeLa S3 cells (Fig. 2*A*, *right panel*). The tissue distribution of AKAP-Lbc protein was determined by immunoblot using antibodies raised against a recombinant fragment encompassing residues 769–1168 of the anchoring protein. A single protein species of ~320 kDa was detected in tissue extracts of human heart but not in the brain or liver (Fig. 2*B*). No bands were detected when the antibody was added in the presence of a 1 μM concentration of the recombinant AKAP-Lbc fragment encompassing residues 769–1168 or when the membranes were incubated with preimmune serum (results not shown). Due to the limited availability of healthy human heart tissues, subcellular fractionation (Fig. 2*C*) and immunocytochemical analyses (Fig. 2*D*) were performed on HeLa S3 cells, which endogenously expressed AKAP-Lbc. HeLa cell lysates were solubilized with increasing concentrations of Triton X-100 or sodium deoxycholate and fractionated by high speed centrifugation. AKAP-Lbc was only detected in deoxycholate fractions (Fig. 2*C*, *lanes 4* and *5*). Immunocytochemical analysis demonstrated that AKAP-Lbc staining (*green*) was uniformly distributed throughout the cells but was excluded from the nucleus (*blue*) (Fig. 2*D*). No signal was detected when the antibody was added in the presence of 1 μM of the recombinant AKAP-Lbc fragment encompassing residues 769–1168 or when

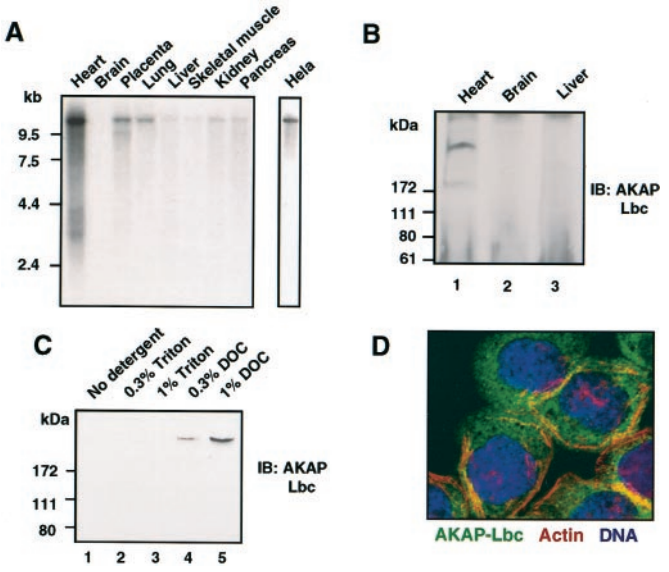

FIG. 2. **Expression and distribution of AKAP-Lbc.** *A*, Northern blot analysis of AKAP-Lbc mRNA expression in human tissues and HeLa cells. A human multiple tissue Northern blot was probed with a fragment encompassing nucleotides 1–500 of the AKAP-Lbc cDNA. A Northern blot of HeLa cell mRNA was probed in parallel. *B*, expression of AKAP-Lbc in different human tissues. AKAP-Lbc was immunoprecipitated from lysates from human heart, brain, and liver. AKAP-Lbc was detected by immunoblot using a polyclonal anti-AKAP-Lbc antibody. *C*, subcellular fractionation of endogenous AKAP-Lbc in HeLa cells. Cells were lysed in the presence of increasing concentrations of Triton X-100 or sodium deoxycholate (*DOC*), soluble proteins were collected and separated by SDS-PAGE (4–15%), and AKAP-Lbc was detected by immunoblot as indicated in *B*. *D*, confocal microscopy of HeLa-S3 cells stained using a polyclonal anti-AKAP-Lbc antibody (*green*), Texas Red phalloidin to detect actin (*red*), and Hoechst dye to detect DNA (*blue*). All of the results are representative of three independent experiments.

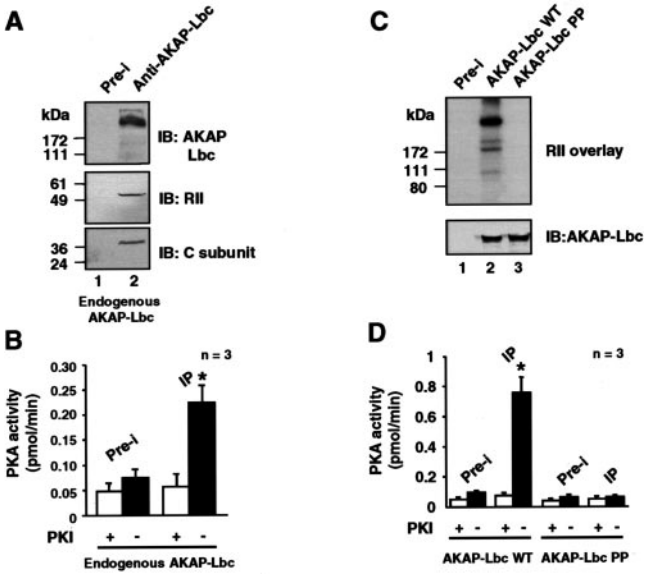

FIG. 3. **AKAP-Lbc binds PKA inside cells.** *A*, HeLa-S3 cell lysates were subjected to immunoprecipitation with either preimmune (*Pre-i*) or affinity-purified anti-AKAP-Lbc antibody. AKAP-Lbc, RII, and the C subunit of PKA (*PKAc*) were then detected by immunoblot using an affinity-purified anti-AKAP-Lbc polyclonal antibody (*upper panel*), a monoclonal anti-RII antibody (*middle panel*), and a monoclonal anti-C subunit antibody (*lower panel*), respectively. The results are representative of three independent experiments. *B*, PKA activity co-immunoprecipitated with endogenous AKAP-Lbc from HeLa-S3 cells. AKAP-Lbc immunoprecipitates were incubated with cAMP (1 mM) and assayed for PKA activity as indicated under "Experimental Procedures." Results are expressed as mean ± S.E. of three independent experiments. Control immunoprecipitates were performed on each sample using preimmune serum (*Pre-i*). Statistical significance was analyzed by paired Student's *t* test. *, $p < 0.05$ as compared with the PKA activity measured in control immunoprecipitates. *C*, HEK293 cells were transfected with AKAP-Lbc or the AKAP-Lbc PP mutant, harvested, and subjected to immunoprecipitation with preimmune serum or affinity-purified anti-AKAP antibody. Immunoprecipitated AKAP-Lbc was detected by immunoblot with an affinity-purified anti-AKAP-Lbc antibody (*lower panel*) or subjected to RII overlay assay (*upper panel*). The results are representative of three independent experiments. *D*, wild type AKAP-Lbc or the AKAP-Lbc PP mutant was immunoprecipitated from transfected HEK293 cells. Control immunoprecipitates were performed on each sample using preimmune serum (*Pre-i*). PKA activity in the immunoprecipitates was measured as described in *B*. Results are expressed as mean ± S.E. of three independent experiments. *, $p < 0.01$ as compared with the PKA activity measured in control immunoprecipitates.

the cells were incubated with preimmune serum (results not shown). These results suggest that AKAP-Lbc is predominantly expressed in the heart and is associated with Triton-insoluble structures within the cytoplasm.

AKAP-Lbc Binds PKA inside Cells—AKAPs are defined as proteins that tether the PKA holoenzyme inside cells (21). Endogenous AKAP-Lbc was immunoprecipitated from HeLa cells (Fig. 3*A*, *top panel*). Both RII (Fig. 3*A*, *middle panel*) and the catalytic subunit of PKA (C subunit) (Fig. 3*A*, *bottom panel*) were co-immunoprecipitated as identified by immunoblot. PKA activity was enriched 3.2 ± 0.5-fold ($n = 3$) upon immunoprecipitation of the anchoring protein when Kemptide was used as a substrate (Fig. 3*B*). Control experiments using preimmune serum did not co-purify PKA subunits or enrich for cAMP-dependent kinase activity (Fig. 3, *A* and *B*). These experiments demonstrate that endogenous AKAP-Lbc and the PKA holoenzyme form a complex inside HeLa cells.

Disruption of the secondary structure within the RII-binding domain of AKAP-Lbc abolished PKA anchoring, as shown by the fact that the AKAP-Lbc PP mutant, in which alanine 1251 and isoleucine 1260 within the PKA anchoring motif were mutated to proline, did not bind RII in the overlay assay (Fig. 3*C*, *top panel*, *lane 3*). In contrast, wild type AKAP-Lbc retained the PKA anchoring function (Fig. 3*C*, *top panel*, *lane 2*). Control experiments demonstrated that equal levels of both AKAP-Lbc forms were immunoprecipitated from HEK293 cells (Fig. 3*C*, *bottom panel*). Furthermore, immunoprecipitation of recombinant AKAP-Lbc enriched kinase activity 15 ± 3.2-fold ($n = 3$) as compared with preimmune control, whereas immunoprecipitation of AKAP-Lbc PP did not (Fig. 3*D*). These data indicate that endogenous and recombinant AKAP-Lbc function as PKA-anchoring proteins inside cells.

AKAP-Lbc Associates with Rho in Vivo—Previous studies have demonstrated that the guanine nucleotide exchange factor Lbc interacts with RhoA in a nucleotide-dependent manner (15, 17, 18). Therefore, we initiated experiments to establish whether AKAP-Lbc binds GTPases of the Rho family. Recombinant AKAP-Lbc was immunoprecipitated from HEK293 cells and incubated with GST fusion proteins of RhoA, Rac1, or Cdc42 (Fig. 4*A*, *lanes 1–3*). AKAP-Lbc only bound to RhoA in its GDP-bound or nucleotide-free conformations (Fig. 4*A*, *lanes 4* and *5*); preloading RhoA with GTPγS abolished the interaction (Fig. 4*A*, *lane 6*). Similar results were obtained with the RhoB and RhoC isoforms (data not shown). AKAP-Lbc interaction with Rac1 and Cdc42 was not detected (Fig. 4*A*, *lanes 7–9* and *10–12*), suggesting that the anchoring protein specifically associates with Rho.

A more rigorous test of this hypothesis was to determine whether AKAP-Lbc retained its specificity for Rho inside cells. Therefore, endogenous AKAP-Lbc was immunoprecipitated

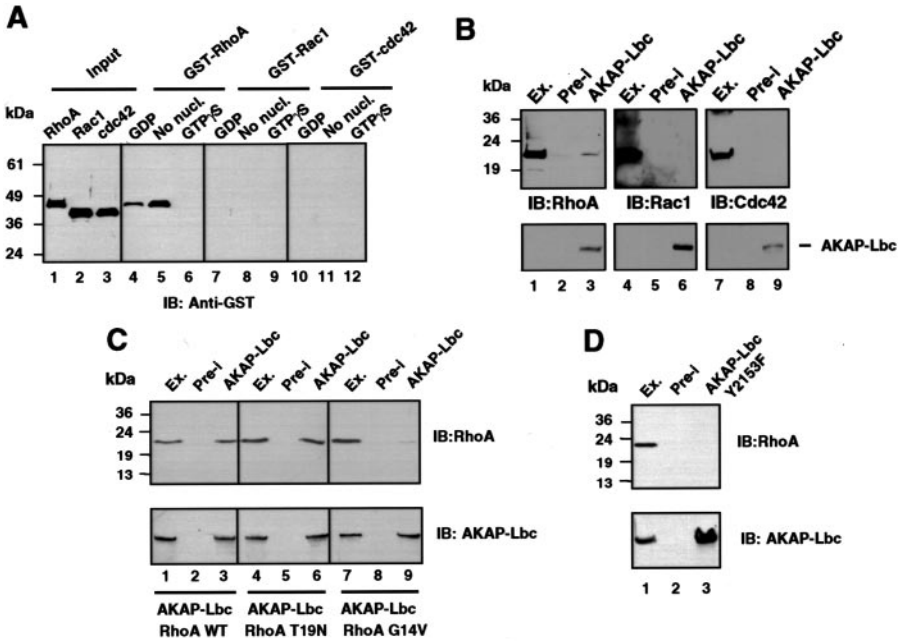

FIG. 4. **AKAP-Lbc associates with Rho *in vivo*.** *A*, AKAP-Lbc was immunoprecipitated from transfected HEK293 cells. Immunoprecipitates were used in an *in vitro* interaction assay to pull down purified GST-RhoA, GST-Rac1, or GST-Cdc42 preloaded with either GDP or GTPγS or nucleotide-depleted (*no nucl.*). RhoA (*lanes 4–6*), Rac1 (*lanes 7–9*), and Cdc42 (*lanes 10–12*) were detected with anti-GST antibody. *B*, lysates from untransfected HeLa-S3 cells were subjected to immunoprecipitation with preimmune serum (*Pre-i*) or affinity-purified anti-AKAP-Lbc antibody. Immunoprecipitates as well as HeLa-S3 cell extracts (*Ex.*) were separated by SDS-PAGE (4–15%) and electrotransferred to nitrocellulose. RhoA, Rac1, and Cdc42 were detected by immunoblot using monoclonal antibodies against RhoA (*lanes 1–3*; *upper panel*), Rac1 (*lanes 4–6*), or Cdc42 (*lanes 7–9*), respectively. AKAP-Lbc was detected with an affinity-purified anti-AKAP-Lbc polyclonal antibody (*lower panel*). *C*, HEK293 cells were transfected with AKAP-Lbc in combination with either wild type (*WT*), constitutively active (*V14*), or dominant negative (*N19*) RhoA. AKAP-Lbc immunoprecipitates as well as cell extracts (*Ex.*) were separated by SDS-PAGE (4–15%) and electrotransferred to nitrocellulose. AKAP-Lbc and RhoA were detected by immunoblot using an affinity-purified anti-AKAP-Lbc antibody (*lower panel*) and a monoclonal anti-RhoA antibody (*upper panel*). *D*, HEK293 cells were transfected with the AKAP-Lbc Y2153F mutant in combination with the cDNA encoding wild-type RhoA. Lysates were subjected to immunoprecipitation with preimmune serum (*Pre-i*) or anti-AKAP-Lbc antibody. RhoA and AKAP-Lbc were detected by immunoblot using a monoclonal anti-RhoA antibody (*upper panel*) or anti-AKAP-Lbc (*lower panel*). All of the results are representative of three independent experiments.

from HeLa lysates. Endogenous RhoA was detected by immunoblot in AKAP-Lbc immunoprecipitates (Fig. 4*B*, *top panel*, *lane 3*) but not in immunocomplexes isolated with preimmune serum (Fig. 4*B*, *top panel*, *lane 2*). Control experiments confirmed that endogenous Rac1 and Cdc42 did not co-precipitate with AKAP-Lbc from HeLa cells (Fig. 4*B*, *top panel*, *lanes 6* and *9*). Immunoblot analyses confirmed that equal levels of AKAP-Lbc were immunoprecipitated in each experiment (Fig. 4*B*, *bottom panel*, *lanes 3*, *6*, and *9*). These experiments establish that AKAP-Lbc specifically interacts with Rho inside cells.

Dominant Negative RhoA Mutants Bind AKAP-Lbc inside Cells—To verify the binding studies described above, RhoA and RhoA mutants were co-expressed with AKAP-Lbc in HEK293 cells. Co-precipitation techniques detected the RhoA T19N mutant with the anchoring protein (Fig. 4*C*, *top panel*, *lane 6*). This mutant cannot bind nucleotides and therefore mimics the nucleotide-depleted conformation (30). In contrast, the RhoA G14V mutant could not be co-precipitated with the anchoring protein (Fig. 4*C*, *top panel*, *lane 9*). This mutant cannot hydrolyze GTP and therefore mimics the GTP-bound state of RhoA (30). These experiments confirm that AKAP-Lbc interacts with nucleotide-depleted or GDP-bound forms of RhoA inside cells. Control experiments demonstrate that equal levels of AKAP-Lbc were immunoprecipitated from HEK293 cells in each binding assay (Fig. 4*C*, *bottom panels*). In reciprocal experiments, we determined whether mutations in AKAP-Lbc could perturb the interaction with RhoA. The QRITKY motif is a characteristic sequence within the DH domain of several Rho guanine nucleotide exchange factors (9). Mutation of the tyrosine within this motif ablates the transforming activity of onco-Lbc (17). Accordingly, mutation of tyrosine 2153 in AKAP-Lbc abolished interaction with RhoA (Fig. 4*D*, *lane 3*). This suggests that tyrosine 2153 within the DH domain of AKAP-Lbc is a determinant for the interaction of AKAP-Lbc with RhoA.

AKAP-Lbc Maintains a Trimeric Complex of Rho and PKA—Endogenous Rho was immunoprecipitated from HEK293 cells using a polyclonal antibody to assess whether AKAP-Lbc can simultaneously associate with the GTPase and PKA (Fig. 5*A*). In fact, RII was present in Rho immunoprecipitations, indicating that the trimeric complex was isolated (Fig. 5*B*, *top panels*). RII was only present in Rho immunocomplexes from cells expressing wild-type AKAP-Lbc (Fig. 5*B*, *top panel*, *lane 6*) and was not detected in immunocomplexes isolated from cells expressing the AKAP-Lbc PP mutant (Fig. 5*B*, *top panel*, *lane 9*). Likewise, Rho-GEF activity was required to form the trimeric complex as immunocomplexes isolated from cells expressing the AKAP-Lbc Tyr^{2153} mutant lacked RII (Fig. 5*B*, *top panel*, *lane 12*). Control experiments confirmed that approximately equal amounts of endogenous RhoA were immunoprecipitated in each case (Fig. 5*B*, *bottom panels*) and that the different AKAP-Lbc mutants were expressed at equivalent levels (data not shown). A more stringent test of this hypothesis was the demonstration that AKAP-Lbc immunocomplexes isolated from human heart extracts contained RII and Rho, whereas experiments with control IgG did not (Fig. 5*C*). These data suggest that AKAP-Lbc functions as an adaptor protein to maintain a signaling complex that includes the PKA holoenzyme and Rho in both transfected cells and heart tissue.

AKAP-Lbc Is a Rho-specific GEF—*In vitro* assays measured the Rho-GEF activity of AKAP-Lbc (Fig. 6*A*). The anchoring

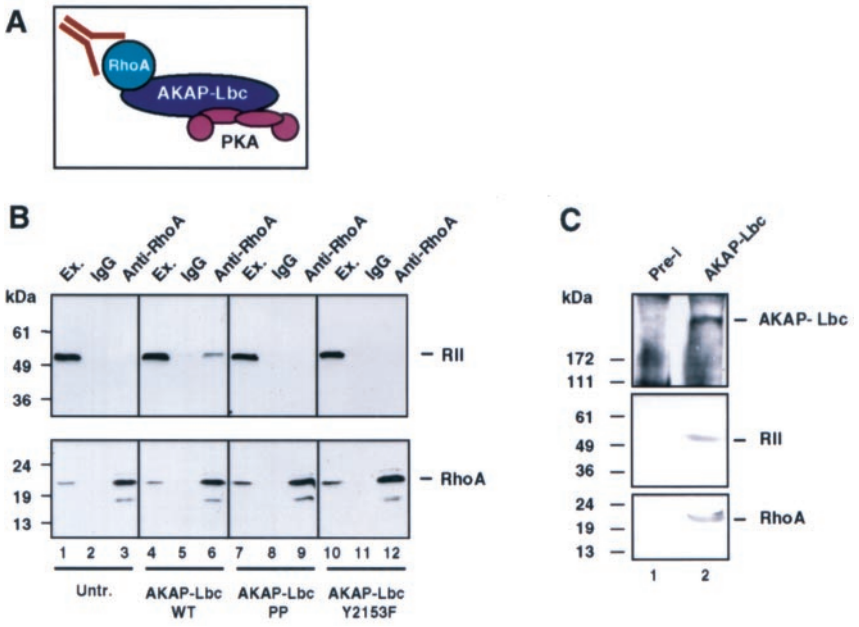

FIG. 5. **AKAP-Lbc, Rho, and PKA form trimeric complexes inside cells.** *A*, model depicting the AKAP-Lbc·PKA·RhoA signaling complex. *B*, HEK293 cells were transfected with either AKAP-Lbc, AKAP-Lbc PP, or AKAP-Lbc Y2153F. Lysates were subjected to immunoprecipitation using either anti-RhoA polyclonal antibodies or nonimmune IgG. Immunoprecipitates as well as cell extracts (*Ex.*) were separated by SDS-PAGE (4–15%) and electrotransferred to nitrocellulose. RhoA and RII were detected by immunoblot using a monoclonal anti-RhoA antibody (*lower panel*) and a monoclonal anti-RII antibody (*upper panel*). *C*, lysates prepared from whole human heart were subjected to immunoprecipitation with preimmune serum (*Pre-i*) or affinity-purified anti-AKAP-Lbc antibody. AKAP-Lbc, RII, and RhoA were detected by immunoblot using an affinity-purified anti-AKAP-Lbc antibody (*upper panel*), a monoclonal anti-RII antibody (*middle panel*), and a monoclonal anti-RhoA antibody (*lower panel*), respectively. All of the results are representative of three independent experiments.

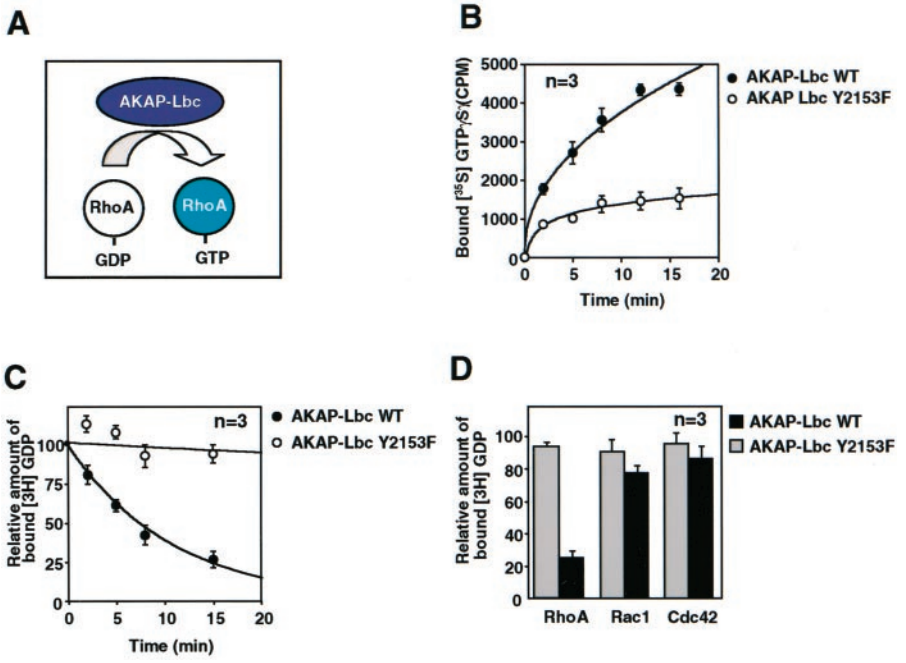

FIG. 6. **AKAP-Lbc is a Rho-specific guanine nucleotide exchange factor.** *A*, model depicting the guanine nucleotide exchange reaction mediated by AKAP-Lbc. *B*, time course for the binding of [^{35}S]GTPγS to purified RhoA. Purified RhoA was preloaded with GDP and then added to reaction incubations containing [^{35}S]GTPγS together with aliquots from HEK293 cell lysates overexpressing AKAP-Lbc (*solid circles*) or the AKAP-Lbc Y2153F mutant (*open circles*). *C*, time course for the dissociation of [^{3}H]GDP from purified RhoA. Purified RhoA was preloaded with [^{3}H]GDP and then added to reaction incubations containing 1 mM GTP together with aliquots from HEK293 cell lysates overexpressing AKAP-Lbc (*solid circles*) or the AKAP-Lbc Y2153F mutant (*open circles*). *D*, effect of AKAP-Lbc on [^{3}H]GDP dissociation from either RhoA Rac1 or Cdc42. Each GTP-binding protein was preloaded with [^{3}H]GDP and then mixed in reaction buffer with extracts overexpressing AKAP-Lbc (*solid bars*) or the AKAP-Lbc Tyr^{2153} mutant (*gray bars*) for 20 min before termination of reactions. Results are expressed as mean ± S.E. of three independent experiments.

protein enhanced the incorporation of [^{35}S]GTPγS into purified RhoA (Fig. 6*B*, *closed circles*), whereas the AKAP-Lbc Y2153F mutant was unable to facilitate this process (Fig. 6*B*, *open circles*). In reciprocal experiments, [^{3}H]GDP dissociation from purified RhoA was enhanced by AKAP-Lbc (Fig. 6*C*, *closed circles*) but not by the AKAP-Lbc Y2153F mutant (Fig. 6*B*, *open circles*). The GDP release assay also confirmed that the guanine nucleotide exchange activity associated with AKAP-Lbc is selective for Rho, since AKAP-Lbc had no effect on the dissociation of GDP from Rac1 or Cdc42 (Fig. 6*D*). In mammalian cells, RhoA induces actin stress fiber formation and focal adhesion assembly (1). The formation of actin stress fibers in NIH-3T3 fibroblasts was used to measure the GEF activity of AKAP-Lbc (Fig. 7, *A–C*). Fibroblasts were transfected with AKAP-Lbc or the AKAP-Lbc Y2153F GEF-defective mutant fused to GFP, serum-starved for 24 h, and then stained with Texas Red-phalloidin to detect F-actin. Control untransfected cells did not contain stress fibers (Fig. 7*D*). Overexpression of AKAP-Lbc induced stress fibers in 35% of the transfected cells (n = 80) (Fig. 7, *A* and *D*). The frequency of cells with stress fibers was dramatically reduced to 5% (n = 74) in cells co-expressing AKAP-Lbc and the Rho inhibitor C3 transferase (Fig. 7, *B* and *D*). Expression of the AKAP-Lbc Y2153F mutant did not induce actin reorganization (n = 78; Fig. 7, *C* and *D*). These results demonstrate that AKAP-Lbc is a Rho-specific guanine nucleotide exchange factor inside cells.

Using the rhotekin capture assay (33), we were able to measure the amount of GTP-bound Rho in produced HEK293 cells expressing AKAP-Lbc, proto-Lbc, or onco-Lbc (Fig. 7, *E* (*top panel*) and *F*). After 24 h of serum starvation, intracellular

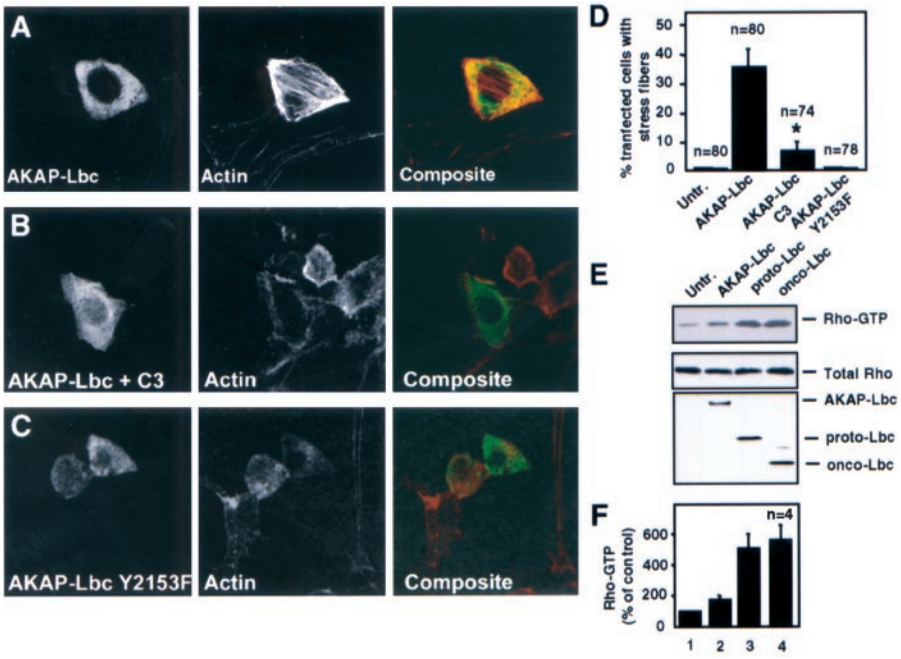

FIG. 7. **AKAP-Lbc induces stress fiber formation in NIH-3T3 fibroblasts.** *A–C*, confocal microscopy of NIH-3T3 fibroblasts transfected with cDNAs encoding for wild type AKAP-Lbc-GFP (*A*), AKAP-Lbc-GFP in combination with the C3 botulinum toxin (*B*), or AKAP-Lbc-GFP Y2153F (*C*). After a 24-h serum starvation, cells were stained using Texas Red phalloidin to detect actin (*middle panels*). The GFP fusion proteins were visualized directly by fluorescent excitation at 488 nm (*left panels*). Merged images are shown in the *right panels*. *D*, frequency of cells with stress fibers in NIH-3T3 cells transfected with either wild type AKAP-Lbc-GFP, AKAP-Lbc-GFP in combination with the C3 botulinum toxin, or the AKAP-Lbc-GFP Y2153F mutant. Values are mean ± S.E. of three independent experiments. For each experimental condition, the total number of analyzed cells is indicated. *E*, HEK293 cells were transfected with AKAP-Lbc, proto-Lbc, or onco-Lbc. After a 24-h serum starvation, cells were harvested, and the lysates were incubated with a GST fusion protein of the RBD of rhotekin. The bound RhoA was detected by immunoblot with a polyclonal anti-RhoA antibody (*upper panel*). The relative amounts of total RhoA, AKAP-Lbc, proto-Lbc, and onco-Lbc in the cell lysates were assessed using polyclonal antibodies against RhoA (*middle panel*) and GFP (*lower panel*), respectively. Results are representative of four independent experiments. *F*, quantitative analysis of the total amount of GTP-RhoA associated with RBD beads was obtained by densitometry. For these experiments, the RhoA bound to RBD (*E*, *upper panel*) was normalized to the total RhoA content of cell extracts (*E*, *middle panel*). Results are expressed as mean ± S.E. of three independent experiments.

GTP-Rho was captured using the GST-Rho binding domain (GST-RBD) fusion protein (Fig. 7*E*, *top panel*). Expression of AKAP-Lbc induced a 1.8 ± 0.3-fold ($n = 4$) increase in Rho-GTP when compared with untransfected HEK293 cells (Fig. 7*F*). In contrast, expression of an equivalent level of onco-Lbc and proto-Lbc (Fig. 7*E*, *bottom panel*) promoted a 5.5 ± 0.9- and 5.1 ± 0.8-fold ($n = 4$) increase in Rho-GTP, respectively (Fig. 7*F*). Control experiments confirmed that equivalent levels of endogenous Rho were present in all cells (Fig. 7*E*, *middle panel*). These results show that AKAP-Lbc possesses a lower basal GEF activity than onco- or proto-Lbc, suggesting that upstream elements might control the activation status of AKAP-Lbc, whereas onco- and proto-Lbc are less regulated. Onco-Lbc has been shown to be oncogenic *in vivo* and to induce transformation of NIH-3T3 cells *in vitro* (15). This transforming activity is dramatically reduced in proto-Lbc, which is virtually unable to transform NIH-3T3 cells *in vitro* (17). Similarly, AKAP-Lbc did not induce formation of transformed foci in transfected NIH-3T3 cells, whereas control experiments with onco-Lbc did form foci, suggesting that AKAP-Lbc has no transforming potential.[2]

AKAP-Lbc Is Activated through a $G\alpha_{12}$-mediated Pathway—LPA and thrombin are extracellular ligands that activate Rho signaling in a variety of cells (34). Agonist-bound LPA or thrombin receptors relay signals to Rho through the heterotrimeric G protein subunits $G\alpha_{12}$ and $G\alpha_{13}$ (7, 34). Using the rhotekin assay as a method to measure Rho activation, we examined which G protein α subunits were involved in the stimulation of AKAP-Lbc activity in HEK293 cells (Fig. 8). Expression of AKAP-Lbc alone induced 1.8 ± 0.3-fold ($n = 3$) increase of GTP-bound Rho, compared with untransfected cells (Fig. 8*A*, *top panel*, *lane 2*). Co-expression of activated $G\alpha_{12}$ with AKAP-Lbc produced a statistically significant increase in GTP-Rho (Fig. 8, *A* (*top panel*, *lane 5*) and *B*). This 7.5 ± 0.8-fold ($n = 3$) increase was greater than the sum of GTP-Rho measured in cells transfected with $G\alpha_{12}$ or AKAP-Lbc alone (Fig. 8, *A* (*upper panel*, *lanes 2* and *4*) and *B*). In all cases, expression of the AKAP-Lbc Y2153F mutant attenuated the accumulation of GTP-Rho (Fig. 8, *A* and *B*). Furthermore, expression of the AKAP-Lbc Y2153F mutant blocked the action of $G\alpha_{12}$ (Fig. 8, *A* (*upper panel*, *lanes 4* and *6*) and *B*). These data suggest that $G\alpha_{12}$ is an upstream activator of AKAP-Lbc in the Rho signaling pathway.

Less robust Rho activation was obtained upon co-expression of AKAP-Lbc with $G\alpha_{13}$ (Fig. 8*B*). Importantly, co-expression of both proteins did not have a synergistic effect on Rho activation, implying that $G\alpha_{13}$ may not activate AKAP-Lbc inside cells. Further controls confirmed that co-expression of AKAP-Lbc with constitutively active $G\alpha_s$, $G\alpha_{i2}$, $G\alpha_q$, or $G\alpha_{11}$ did not further increase the GEF activity of the anchoring protein (Fig. 8*A*, *top panels*, *lanes 10–21*). Immunoblotting confirmed that equal levels of endogenous Rho were present in each cell (Fig. 8*A*, *middle panels*) and that each $G\alpha$ subunit was expressed at the same levels (Fig. 8*A*, *bottom panel*). Collectively, these data suggest that $G\alpha_{12}$ activates AKAP-Lbc in HEK293 cells.

AKAP-Lbc Couples $G\alpha_{12}$ to Rho inside Cells—HEK293 cells contain endogenous LPA receptors, $G\alpha_{12}$ and Rho. These cells were transfected with AKAP-Lbc to recapitulate a Rho activa-

[2] D. Diviani and J. D. Scott, unpublished observations.

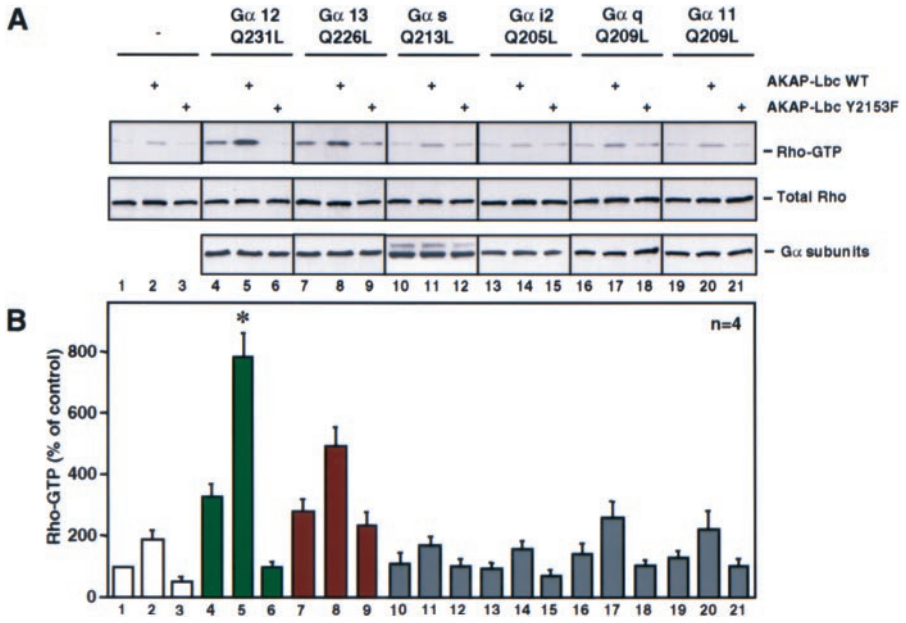

FIG. 8. **$G\alpha_{12}$ activates AKAP-Lbc inside cells.** *A*, HEK293 cells were transfected with AKAP-Lbc or AKAP-Lbc Y2153F alone or in combination with the constitutively active mutants of $G\alpha_{12}$, $G\alpha_{13}$, $G\alpha_s$, $G\alpha_{i2}$, $G\alpha_q$, or $G\alpha_{11}$. After a 24-h serum starvation, cells were harvested, and the lysates were incubated with GST-RBD beads. The bound RhoA was detected with a polyclonal anti-RhoA antibody (*upper panel*). The relative amounts of total RhoA and G protein α subunits in the cell lysates were detected using a polyclonal anti-RhoA rabbit antibody (*middle panel*) and polyclonal antibodies raised against the various α subunits (*lower panel*). Results are representative of three independent experiments. *B*, the total amount of GTP-RhoA associated with RBD beads was quantitated as indicated in Fig. 7*F*. Results are expressed as mean ± S.E. of three independent experiments.

tion pathway *in vivo*. Overexpression of AKAP-Lbc enhanced LPA-induced activation of Rho as measured by the rhotekin capture assay (Fig. 9, *A* (*top panel*, *lanes 4* and *5*) and *B*). In contrast, expression of the GEF-defective mutant, AKAP-Lbc Y2153F, blocked LPA-induced Rho activation (Fig. 9, *A* (*top panel*, *lane 6*) and *B*). Furthermore, expression of the dominant negative mutant, $G\alpha_{12}$ G228A (34), blocked LPA-mediated activation of AKAP-Lbc (Fig. 9, *A* (*top panel*, *lane 8*) and *B*). This inhibitory effect was specific, since overexpression of the dominant negative mutant, $G\alpha_{13}$ G225A, did not significantly inhibit AKAP-Lbc activation (Fig. 9, *A* (*top panel*, *lane 11*) and *B*). Equal levels of endogenous Rho were expressed in all conditions (Fig. 9*A*, *middle panels*). Control experiments showed that overexpression of activated $G\alpha_{12}$ did not significantly increase Rho-GEF activity of proto- and onco-Lbc (Fig. 9*C*, *top panel*, *lanes 6* and *8*). Similarly, the activity of proto- and onco-Lbc could not be enhanced by treatment of cells with LPA (results not shown). Since the extent of Rho activation measured in serum-starved cells expressing proto- or onco-Lbc (Fig. 9*C*, *top panel*, *lanes 5* and *7*) was comparable with that observed in cells expressing both AKAP-Lbc and $G\alpha_{12}$ active mutant (Fig. 9*C*, *top panel*, *lane 4*), these results suggest that proto- and onco-Lbc might already be in an active state under basal conditions.

Finally, AKAP-Lbc was immunoprecipitated from cells co-expressing the dominant active $G\alpha_{12}$ Q231L mutant. Recombinant $G\alpha_{12}$ was detected by immunoblot in AKAP-Lbc immunocomplexes (Fig. 9*D*, *lane 3*). Control experiments demonstrated that $G\alpha_{12}$ was not present in immunocomplexes isolated with preimmune IgG (Fig. 9*D*, *lane 2*). Reciprocal experiments confirmed this interaction when AKAP-Lbc was detected by Western blot in $G\alpha_{12}$ immunocomplexes (Fig. 9*E*, *lane 3*). AKAP-Lbc was not detected in immunocomplexes isolated with control IgG (Fig. 9*E*, *lane 2*). Collectively, these results indicate that AKAP-Lbc is a $G\alpha_{12}$-activated Rho-specific guanine nucleotide exchange factor that responds to LPA. Furthermore, these data suggest that a signaling complex is formed between the active $G\alpha_{12}$ and the anchoring protein.

DISCUSSION

In this report, we show that AKAP-Lbc is a protein kinase A-anchoring protein that also functions as a scaffolding protein to coordinate a Rho signaling pathway. The modular composition of the protein includes an amino-terminal PKA anchoring site fused to a guanine nucleotide Rho-specific exchange factor. This provides a mechanism to compartmentalize cAMP and Rho signaling events within the same macromolecular signaling complex.

Our present findings indicate that AKAP-Lbc is activated in response to LPA-induced stimulation of $G\alpha_{12}$ and are consistent with a role for AKAP-Lbc in Rho-mediated actin reorganization events. This is highlighted in our model (Fig. 10). Inactive Rho binds to AKAP-Lbc in a manner that requires an intact DH domain. Upon stimulation by LPA, $G\alpha_{12}$ is released from sites close to the membrane and induces AKAP-Lbc activation. This allows an intrinsic guanine nucleotide exchange activity residing within the anchoring protein to facilitate the activation of GTP-Rho. Active Rho then participates in various cellular processes, including stress fiber formation (Fig. 10). AKAP-Lbc is central to this process as it provides a scaffold for the transient assembly of this Rho signaling pathway. This conclusion is supported by our cell-based studies showing that expression of AKAP-Lbc promotes the formation of actin stress fibers in fibroblasts.

One intriguing outcome was our observation that AKAP-Lbc appears to be preferentially activated by $G\alpha_{12}$ compared with $G\alpha_{13}$. Co-expressed $G\alpha_{12}$ and AKAP-Lbc act synergistically to increase cellular levels of GTP-Rho, whereas a dominant negative mutant of $G\alpha_{12}$, but not of $G\alpha_{13}$, blocks the LPA-induced activation of AKAP-Lbc. This suggests that in HEK293 cells, LPA-induced activation of AKAP-Lbc is preferentially mediated by $G\alpha_{12}$. Previous findings indicated that in Swiss-3T3 cells, LPA stimulates Rho signaling through activation of $G\alpha_{13}$ (34, 35). However, in agreement with our observation that LPA can signal to $G\alpha_{12}$, recent evidence indicates that LPA-induced activation of Rho is blocked in $G\alpha_{12}$ knockout mice.[3] The apparent discrepancy between these findings might be explained by the presence of LPA receptor subtypes with distinct coupling selectivities in different cell types. Additionally, we have been able to co-precipitate recombinant $G\alpha_{12}$ Q213L dominant active mutant with AKAP-Lbc when both proteins are expressed in HEK293 cells, suggesting that a signaling complex is formed between the active $G\alpha_{12}$ and the anchoring protein. These

[3] M. I. Simon, personal communication.

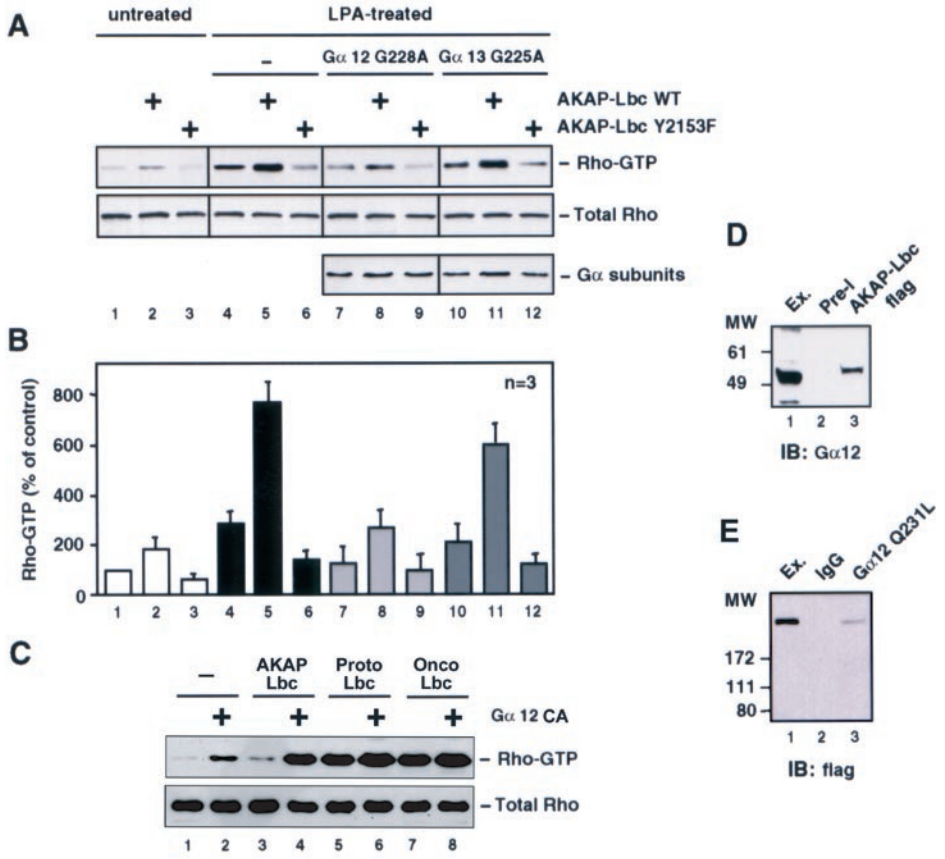

FIG. 9. **LPA activates AKAP-Lbc through a $G\alpha_{12}$-mediated signaling pathway.** *A*, HEK293 cells were transfected with AKAP-Lbc or AKAP-Lbc Y2153F alone or in combination with the dominant negative mutant of $G\alpha_{12}$ or $G\alpha_{13}$. After a 24-h serum starvation, cells were incubated for 5 min in the absence or presence of 10 μM LPA. Cells were then harvested, and the lysates were incubated with GST-RBD beads. RBD-bound RhoA, total RhoA, and G protein α subunits in the cell lysate were detected as indicated in the legend to Fig. 8*A*. Results are representative of three independent experiments. *B*, the total amount of GTP-RhoA associated with RBD beads was quantitated as indicated in the legend of Fig. 7*F*. Results are expressed as mean ± S.E. of three independent experiments. *C*, HEK293 cells were transfected with AKAP-Lbc, proto-Lbc, or onco-Lbc alone or in combination with the constitutively active mutant of $G\alpha_{12}$ ($G\alpha_{12}$CA). After a 24-h serum starvation, cells were harvested, and the lysates were incubated with GST-RBD beads. RBD-bound RhoA and total RhoA in the cell lysate were detected as indicated in the legend to Fig. 8*A*. Results are representative of three independent experiments. *D*, HEK293 cells were transfected with FLAG-tagged AKAP-Lbc in combination with the constitutively active mutant of $G\alpha_{12}$ (Q231L). Immunoprecipitations were performed using either anti-FLAG antibodies or nonimmune IgG. The $G\alpha_{12}$ Q231L mutant was detected by immunoblot using a polyclonal anti-$G\alpha_{12}$ antibody. *E*, HEK293 cells were transfected with FLAG-tagged AKAP-Lbc in combination with the constitutively active mutant of $G\alpha_{12}$ (Q231L). Immunoprecipitations were performed using either an anti-$G\alpha_{12}$ polyclonal antibody or nonimmune IgG. AKAP-Lbc was detected by immunoblot using anti-FLAG antibody. Results are representative of three independent experiments.

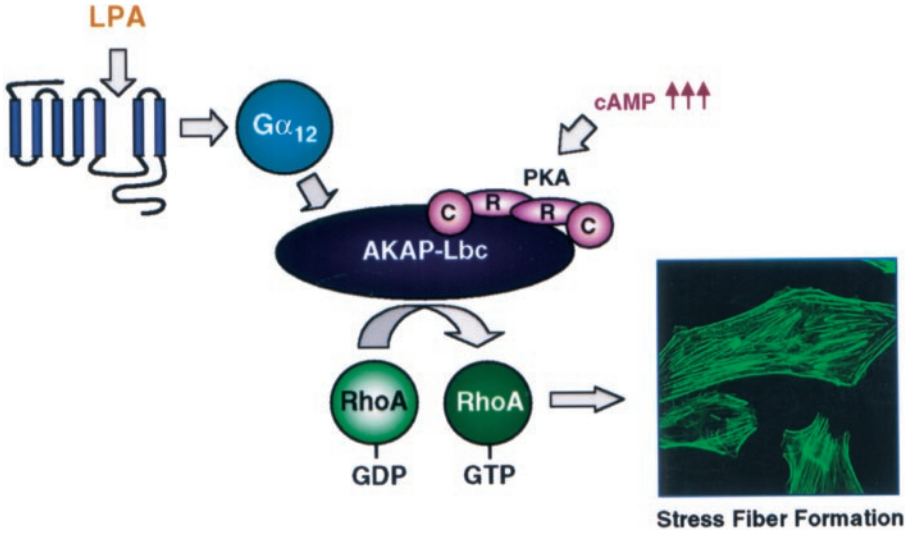

FIG. 10. **Model for the AKAP-Lbc signaling complex.** The AKAP-Lbc-PKA complex is activated in response to LPA stimulation through a $G\alpha_{12}$-mediated signaling pathway. Activated AKAP-Lbc interacts with Rho through its DH domain and induces the exchange of GDP for GTP. GTP-bound Rho is released from the AKAP-Lbc-PKA complex, interacts with downstream effectors, and induces actin stress fiber formation.

interactions are most likely transient, since isolation of the endogenous complex from HeLa cells was inconsistent. The molecular mechanisms involved in the activation of AKAP-Lbc appear to be distinct from other guanine nucleotide exchange factors such as p115 Rho-GEF, which preferentially interacts with $G\alpha_{13}$ through an RGS-like domain inside cells (10, 11).

AKAP-Lbc does not contain an RGS domain, suggesting that another protein must be present in the signaling complex to provide GTPase activating activity. Current studies are focusing on identifying other AKAP-Lbc binding partners.

Our immunocytochemical analyses indicate that AKAP-Lbc is distributed throughout the cell, and subcellular fractionation data suggest that it is enriched in deoxycholate-soluble fractions. Immunofluorescent images presented in Fig. 7*A* indicate that an AKAP-Lbc-GFP does not align with actin stress fibers in NIH-3T3 fibroblasts. Interestingly, Rho activation signals promote the movement of onco-Lbc to the stress fibers (36). The differential location of the onco- and AKAP-Lbc proteins may be explained by interaction with different binding partners. This may involve the unique amino-terminal region of the anchoring protein, which contains additional protein interaction modules such as ankyrin repeats. Our activity measurements also indicate that AKAP-Lbc has a lower basal Rho-GEF activity than onco- or proto-Lbc (Fig. 7*E*). One explanation is that NH_2-terminal inhibitory sequences of AKAP-Lbc residing upstream of the Lbc region maintain intramolecular interactions that maintain a low level of tonic GEF activity. A similar model has been proposed for the regulation the Dbl and Vav families of guanine nucleotide exchange factors (37, 38). For example, an autoinhibitory site in the amino terminus of the exchange factor Vav attenuates GEF activity through interactions with the DH domain (38). Tyrosine phosphorylation of Tyr^{174} by Lck stimulates GEF activity by relieving autoinhibitory contact with the DH domain (39, 40). While onco- and proto-Lbc display very different transforming activities in NIH-3T3 cells (15, 17, 18), their GEF activities are comparable (Fig. 7*E*). This is in agreement with previous observations showing that in COS-7 cells onco- and proto-Lbc possess similar Rho-GEF activities (15, 17, 18). This suggests that nucleotide exchange activity alone is not sufficient to account for the biological difference between onco- and proto-Lbc.

The RII binding site of the Ht31 fragment has served as the prototype for the development of the PKA anchoring hypothesis, which suggests that amphipathic helices on AKAPs bind to the RII dimer of the PKA holoenzyme (29). 10 years after these initial reports, we now demonstrate that the parent molecule, AKAP-Lbc, is a guanine nucleotide exchange factor associated with an anchored pool of PKA. This suggests that the cAMP and Rho signaling pathways are compartmentalized within the AKAP-Lbc signaling complex. However, dissecting the interplay between both pathways may prove to be complicated. Previous reports have suggested that forskolin treatment prevents stress fiber formation and that PKA phosphorylation of Ser^{188} of RhoA inhibits association with Rho-kinase (41–43). However, we have been unable to demonstrate increased PKA phosphorylation of Rho in cells transfected with AKAP-Lbc.[2] Another possibility could be that PKA anchoring facilitates phosphorylation of the anchoring protein itself. However, AKAP-Lbc is not phosphorylated by the kinase *in vitro* or inside cells.[2] We could also show that wild type AKAP-Lbc and PKA anchoring-deficient mutant of AKAP-Lbc (AKAP-Lbc PP) display similar Rho-GEF activities both *in vitro* and inside cells. This suggests that the anchored PKA does not influence the ability of AKAP-Lbc to activate Rho. At this time, we have not established a link between PKA anchoring and the assembly of a Rho signaling pathway on AKAP-Lbc. One possibility is that PKA affects the phosphorylation of as yet unidentified substrates that may be recruited into the Rho signaling scaffold. Alternatively, AKAP-Lbc may provide a molecular platform for the localization of Rho and PKA, which may function in parallel but functionally distinct signaling pathways (Fig. 10). Similarly, another AKAP, WAVE-1, assembles an actin-based signaling complex including PKA and the tyrosine kinase Abl in response to signals transduced by a related GTPase Rac (44, 45). Also, the mammalian PAR-3-PAR-6 complex binds Cdc42 or Rac and atypical PKC isoforms to form a signaling complex that participates in the maintenance of cell polarity (46–48). Thus, AKAP-Lbc is a member of an emerging class of anchoring proteins that coordinate the location of Rho GTPases with second messenger-regulated protein kinases.

In conclusion, there are several important implications of this study. AKAP-Lbc is a chimeric protein that is an A-kinase-anchoring protein and a novel splice variant of the guanine nucleotide exchange factor Lbc. Our studies suggest that the guanine nucleotide exchange activity of AKAP-Lbc is specifically stimulated by the heterotrimeric G protein α subunit $G\alpha_{12}$ in response to signals emanating from the LPA receptor. Ongoing studies are focusing on identifying additional components of the AKAP-Lbc signaling complex and characterizing the functional role of the AKAP-Lbc-mediated anchoring of PKA.

Acknowledgments—We thank Lorene Langeberg for assistance in the preparation of the manuscript, Robert Mouton for excellent technical assistance, and colleagues at the Scott laboratory for critically evaluating the manuscript.

REFERENCES

1. Hall, A. (1998) *Science* **279,** 509–514
2. Bishop, A. L., and Hall, A. (2000) *Biochem. J.* **348,** 241–255
3. Hill, C. S., and Treisman, R. (1995) *Cell* **80,** 199–211
4. Hill, C. S., Wynne, J., and Treisman, R. (1995) *Cell* **81,** 1159–1170
5. Olson, M. F., Ashworth, A., and Hall, A. (1995) *Science* **269,** 1270–1272
6. Strathmann, M. P., and Simon, M. I. (1991) *Proc. Natl. Acad. Sci. U. S. A.* **88,** 5582–5586
7. Buhl, A. M., Johnson, N. L., Dhanasekaran, N., and Johnson, G. L. (1995) *J. Biol. Chem.* **270,** 24631–24634
8. Kaibuchi, K., Kuroda, S., and Amano, M. (1999) *Annu. Rev. Biochem.* **68,** 459–486
9. Cerione, R. A., and Zheng, Y. (1996) *Curr. Opin. Cell Biol.* **8,** 216–222
10. Kozasa, T., Jiang, X., Hart, M. J., Sternweis, P. M., Singer, W. D., Gilman, A. G., Bollag, G., and Sternweis, P. C. (1998) *Science* **280,** 2109–2111
11. Hart, M. J., Jiang, X., Kozasa, T., Roscoe, W., Singer, W. D., Gilman, A. G., Sternweis, P. C., and Bollag, G. (1998) *Science* **280,** 2112–2114
12. Fukuhara, S., Murga, C., Zohar, M., Igishi, T., and Gutkind, J. S. (1999) *J. Biol. Chem.* **274,** 5868–5879
13. Togashi, H., Nagata, K., Takagishi, M., Saitoh, N., and Inagaki, M. (2000) *J. Biol. Chem.* **275,** 29570–29578
14. Jackson, M., Song, W., Liu, M. Y., Jin, L., Dykes-Hoberg, M., Lin, C. I., Bowers, W. J., Federoff, H. J., Sternweis, P. C., and Rothstein, J. D. (2001) *Nature* **410,** 89–93
15. Toksoz, D., and Williams, D. A. (1994) *Oncogene* **9,** 621–628
16. Zheng, Y., Olson, M. F., Hall, A., Cerione, R. A., and Toksoz, D. (1995) *J. Biol. Chem.* **270,** 9031–9034
17. Sterpetti, P., Hack, A. A., Bashar, M. P., Park, B., Cheng, S. D., Knoll, J. H., Urano, T., Feig, L. A., and Toksoz, D. (1999) *Mol. Cell. Biol.* **19,** 1334–1345
18. Rubino, D., Driggers, P., Arbit, D., Kemp, L., Miller, B., Coso, O., Pagliai, K., Gray, K., Gutkind, S., and Segars, J. (1998) *Oncogene* **16,** 2513–2526
19. Colledge, M., and Scott, J. D. (1999) *Trends Cell Biol.* **9,** 216–221
20. Scott, J. D., and Pawson, T. (2000) *Sci. Am.* **282,** 72–79
21. Diviani, D., and Scott, J. D. (2001) *J. Cell Sci.* **114,** 1431–1437
22. Dodge, K. L., Khouangsathiene, S., Kapiloff, M. S., Mouton, R., Hill, E. V., Houslay, M. D., Langeberg, L. K., and Scott, J. D. (2001) *EMBO J.* **20,** 1921–1930
23. Klauck, T. M., Faux, M. C., Labudda, K., Langeberg, L. K., Jaken, S., and Scott, J. D. (1996) *Science* **271,** 1589–1592
24. Nauert, J. B., Klauck, T. M., Langeberg, L. K., and Scott, J. D. (1997) *Curr. Biol.* **7,** 52–62
25. Takahashi, M., Shibata, H., Shimakawa, M., Miyamoto, M., Mukai, H., and Ono, Y. (1999) *J. Biol. Chem.* **274,** 17267–17274
26. Takahashi, M., Mukai, H., Oishi, K., Isagawa, T., and Ono, Y. (2000) *J. Biol. Chem.* **275,** 34592–34596
27. Carr, D. W., Stofko-Hahn, R. E., Fraser, I. D. C., Bishop, S. M., Acott, T. S., Brennan, R. G., and Scott, J. D. (1991) *J. Biol. Chem.* **266,** 14188–14192
28. Newlon, M. G., Roy, M., Morikis, D., Carr, D. W., Westphal, R., Scott, J. D., and Jennings, P. A. (2001) *EMBO J.* **20,** 1651–1662
29. Carr, D. W., Hausken, Z. E., Fraser, I. D. C., Stofko-Hahn, R. E., and Scott, J. D. (1992) *J. Biol. Chem.* **267,** 13376–13382
30. Self, A. J., and Hall, A. (1995) *Methods Enzymol.* **256,** 67–76
31. Corbin, J. D., and Reimann, E. M. (1974) *Methods Enzymol.* **38,** 287–294
32. Zheng, Y., Hart, M. J., and Cerione, R. A. (1995) *Methods Enzymol.* **256,** 77–84
33. Ren, X. D., and Schwartz, M. A. (2000) *Methods Enzymol.* **325,** 264–272
34. Gohla, A., Offermanns, S., Wilkie, T. M., and Schultz, G. (1999) *J. Biol. Chem.* **274,** 17901–17907
35. Gohla, A., Harhammer, R., and Schultz, G. (1998) *J. Biol. Chem.* **273,** 4653–4659
36. Olson, M. F., Sterpetti, P., Nagata, K., Toksoz, D., and Hall, A. (1997) *Onco-*

gene **15,** 2827–2831
37. Bi, F., Debreceni, B., Zhu, K., Salani, B., Eva, A., and Zheng, Y. (2001) *Mol. Cell. Biol.* **21,** 1463–1474
38. Aghazadeh, B., Lowry, W. E., Huang, X. Y., and Rosen, M. K. (2000) *Cell* **102,** 625–633
39. Brunati, A. M., Donella-Deana, A., Ruzzene, M., Marin, O., and Pinna, L. A. (1995) *FEBS Lett.* **367,** 149–152
40. Han, J., Das, B., Wei, W., Van Aelst, L., Mosteller, R. D., Khosravi-Far, R., Westwick, J. K., Der, C. J., and Broek, D. (1997) *Mol. Cell. Biol.* **17,** 1346–1353
41. Lang, P., Gesbert, F., Delespine-Carmagnat, M., Stancou, R., Pouchelet, M., and Bertoglio, J. (1996) *EMBO J.* **15,** 510–519
42. Busca, R., Bertolotto, C., Abbe, P., Englaro, W., Ishizaki, T., Narumiya, S., Boquet, P., Ortonne, J. P., and Ballotti, R. (1998) *Mol. Biol. Cell* **9,** 1367–1378
43. Dong, J. M., Leung, T., Manser, E., and Lim, L. (1998) *J. Biol. Chem.* **273,** 22554–22562
44. Westphal, R. S., Soderling, S. H., Alto, N. M., Langeberg, L. K., and Scott, J. D. (2000) *EMBO J.* **19,** 4589–4600
45. Takenawa, T., and Miki, H. (2001) *J. Cell Sci.* **114,** 1801–1809
46. Lin, D., Edwards, A. S., Fawcett, J. P., Mbamalu, G., Scott, J. D., and Pawson, T. (2000) *Nat. Cell Biol.* **2,** 540–547
47. Joberty, G., Petersen, C., Gao, L., and Macara, I. G. (2000) *Nat. Cell Biol.* **2,** 531–539
48. Qiu, R. G., Abo, A., and Steven Martin, G. (2000) *Curr. Biol.* **10,** 697–707